SciEn
Journal of Engineering Advancements Vol. 05(02) 2024, pp 35-50 https://doi.org/10.38032/jea.2024.02.002

Computational Study and Analysis of Carotid Artery Stenosis

Toukir Ahmed Chowdhury[*] and Prasanjit Das

Department of Mechanical Engineering, Chittagong University of Engineering & Technology, Chattogram, Bangladesh

Received: October 20, 2023, Revised: May 31, 2024, Accepted: June 05, 2024, Available Online: June 27, 2024

ABSTRACT

Heart diseases and strokes have been the major causes of death both nationally and globally in recent years. Carotid artery stenosis is one of the leading causes of these disorders, along with many others. The constriction of the carotid artery, which provides blood to the head, face, and brain, causes this condition. This constriction happens due to a plaque buildup in the walls of the artery, a condition called atherosclerosis. A computational study on different degrees of stenosis on an artery, mild stenosis (30% stenotic artery) and moderate stenosis (70% stenotic artery) helps to analyze the blood flow patterns and behavior, identify different factors that may vary due to stenosis like – wall shear stress, velocity profile, and pressure distribution. The viscosity coefficient of blood, a non-Newtonian fluid, depends on the shear rate. Two non-Newtonian fluid flow models, Carreau and Cross models, are taken into account for its analysis, and the numerical computation was carried out using ANSYS WORKBENCH ACADEMIC STUDENT 2022 R2 with user-defined function for pulsatile blood flow consideration. This study is expected to aid physicians and medical practitioners, as it shows the proportional relation between pressure and stenosis severity, identifies the more stenosis-prone areas through analysis, and personalizes treatment plans. It also depicts how the Cross model predicts higher WSS values compared to the Carreau model, and so has more reliability for higher severity of stenosis.

Keywords: Hemodynamics, Computational Fluid Dynamics, Blood Flow, Carotid Artery Stenosis, Atherosclerosis.

1 Introduction

In the realm of fluid dynamics, blood behaves as a non-Newtonian fluid, exhibiting unique viscosity and flow properties under varying conditions. It is a unique bodily fluid having red blood cells, white blood cells, platelets, and plasma. This fluid serves the dual function of removing metabolic waste from cells and providing them with essential nutrients. The functionality of a cardiovascular system depends on the continuous flow of blood through the heart. Any kind of abnormalities in its flow can cause fatal consequences. According to a World Health Organization (WHO) report, heart disease and stroke were the top two major causes of mortality and morbidity globally from 2000 to 2019 [1]. A person suffers from a stroke every 40 seconds in the United States. In 2018, the leading causes of mortality in Bangladesh were heart disorders and heart attacks [2]. A report by the Bangladesh Bureau of Statistics (BBS) in 2020 found a total of 21.1% and around 10% of deaths caused due to cardiac arrest and brain stroke respectively [3]. Cardiovascular diseases are causing fatalities all over the globe without any warning signal.

The carotid artery bifurcation is the region where the majority of ischemic strokes initiate. Fig. 1 depicts the branching of the common carotid artery (CCA) into two parts. Fig. 2 displays the major global causes of mortality between the years 2000 and 2019 as stated by the World Health Organization (WHO).

The biomechanics of different vascular diseases can be understood through the study of stenosis. In a healthy artery, blood flows without any complexity. Nevertheless, due to the existence of calcium, cholesterol, and other substances in the bloodstream, a fatty substance called plaque can develop near the inner lining of the artery. It then causes the artery wall to harden with time, a condition known as atherosclerosis. So, the artery wall stops being elastic, which reduces the blood flow area. Arterial stenosis is the medical term for this artery narrowing. The femoral, carotid, and coronary arteries are where it occurs most frequently. Fig. 3 depicts both a healthy artery and an artery constricted by atherosclerotic plaque. Fig. 4 shows the position of the carotid artery and the impact of its stenosis.

Computational Fluid Dynamics (CFD) is an increasingly popular approach for analyzing fluid movements in various conventional and unique contexts. It has several advantages over traditional experimental fluid dynamics (EFD). The first one lies in the time taken for the design and development. Even a simple analysis done experimentally requires time for design, modeling, and setup, which is not the case for CFD. The variation of results can be easily interpreted for alterations in the parameters using CFD. A simple simulation in CFD can demonstrate more detailed results than the other methods. The cost of setup and experiment can easily be avoided if CFD is used.

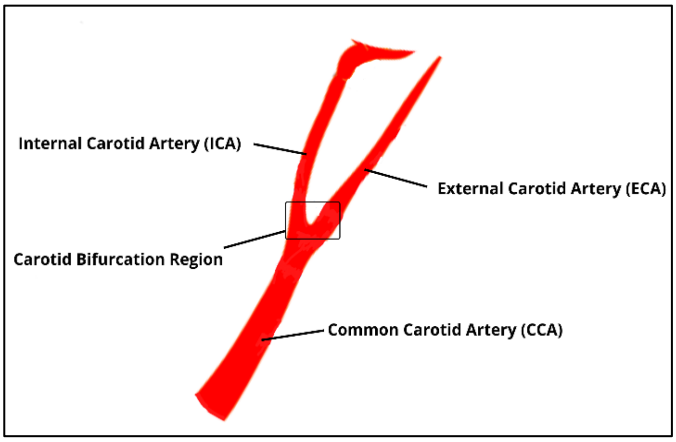

Fig. 1 Schematic diagram of a carotid artery

*Corresponding Author Email Address: toukirac96@gmail.com

Though experimental methods are important in research and the data collected through experiments can be used to validate simulation results, CFD is an economically viable option when the small degree of inaccuracy is taken into account. Several authors have used CFD to solve and analyze blood flow problems. It serves as a dependable technique for assessing hemodynamic parameters, as it can generate results aligning with those from in-vivo research, such as studies by Köhler *et al.* [6], Marshall *et al.* [7] and Tu *et al.* [8], all without the constraints, specialized tools, or substantial expenses associated with the latter methods.

Atherosclerosis leads to a reduction in the elasticity of the arterial wall, narrowing the area through which blood can flow. Khader and Shenoy [9] illustrated this altered blood flow pattern. Furthermore, Li *et al.* [10] found that vessels experiencing consistent blood flow and low shear stress tend to remain relatively free from diseases.

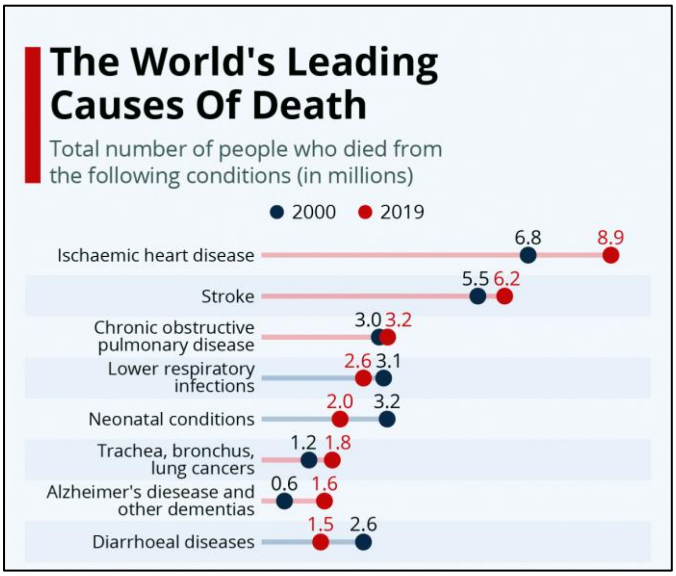

Fig. 2 Leading causes of death in the world between 2000 and 2019 [1]

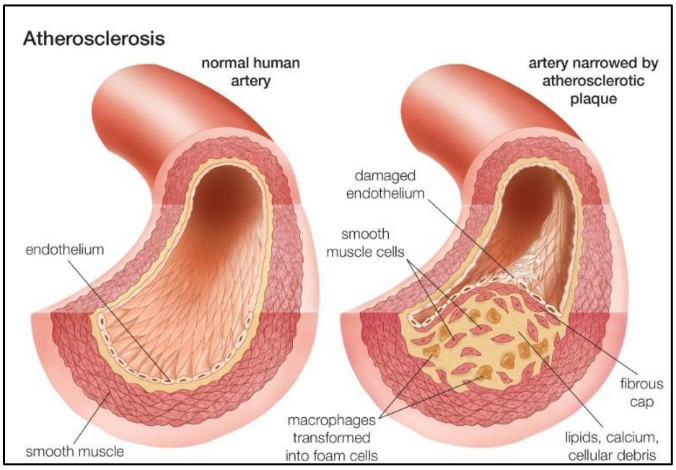

Fig. 3 A normal artery vs. an atherosclerotic artery [4]

According to Chua and Shread [11], in order to assess how critical the stenosis is, physicians examine the patient's symptoms, growth pace, constriction size, and pressure drop. By comparing the stenosed flow behavior with a healthy one, numerical simulation is able to accurately determine the severity findings and provide a proper knowledge of the mechanism of plaque formation, which is an advantage over traditional methods such as MRI, CT, and ultrasound techniques.

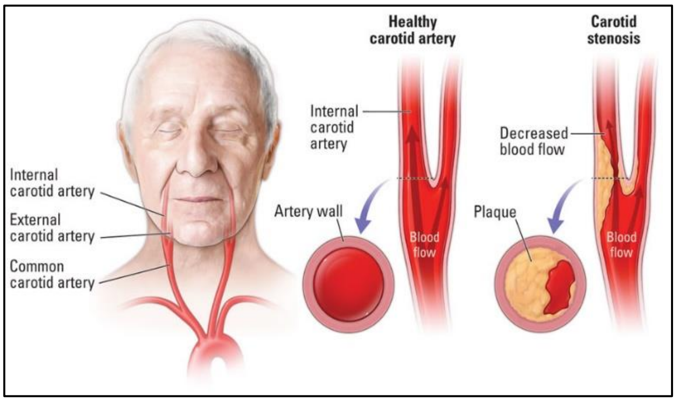

Fig. 4 Carotid artery stenosis [5]

Young *et al.* [12] found that the greatest WSS occurred shortly before the minimum lumen point. Lorenzini and Casalena [13] investigated the non-Newtonian behavior of stenosis with trapezoidal, semi-elliptic, and triangular shapes. There are three types of non-Newtonian blood properties that have been studied: thixotropy, viscoelasticity, and shear thinning. Mandal [14] found that shear thinning is the dominant characteristic of blood among those studied. Cho *et al.* [15] and Johnston *et al.* [16], found the Carreau model effective in producing accurate representations of experimental blood flow conditions. In a study by Gijsen *et al.* [17], it was discovered that choosing the appropriate Reynolds number allowed for a good simulation of the non-Newtonian fluid's flow characteristics. As preliminary research, Formaggia *et al.* [18] and Lee and Xu [19] looked at the blood flow dynamics in normal or non-stenotic arteries. Many theoretical investigations of blood flow across stenosed arteries have lately been conducted. These are summarized in Table 1. Table 1 shows that the majority of studies on carotid artery stenosis conducted to date, with the exception of Salman *et al.* [20] and Bouteloup *et al.* [21], consider the flow type to be laminar. Out of 19 studies included in Table 1, 11 assumed the Newtonian viscosity model, two assumed non-Newtonian, and the remaining six assumed both Newtonian and non-Newtonian flow. The stenotic artery was studied in 12 of these papers.

Many of the previously done research consider blood as a Newtonian fluid to analyze its viscosity models. This assumption may be valid in the case of a healthy carotid artery, but in the case of a stenosed artery, significant changes in parameters such as wall shear stress, velocity distribution, pressure-gradient, and so on may occur due to modeling blood as a non-Newtonian fluid, which is more realistic. Besides, Table 1 shows that most of the previous studies assume laminar flow simulation in carotid arteries. Though this assumption is valid for a healthy artery, a stenosed artery will possibly be more on the transitional or turbulent side of the flow. Furthermore, the arterial geometries considered in the previous studies were mostly simple and non-realistic. Therefore, the comparison of flow behavior in stenosed arteries amongst patients of different ages, genders, etc. could not be done.

In this study, two degrees of stenosis in a carotid artery are considered for simulation. The geometries are constructed using SolidWorks 2020. The simulation of the geometry for blood flowing through the artery is continued using simulation software.

Table 1 Carotid artery CFD numerical studies from 2016 to 2022

References	Year	Flow type	Viscosity model	Stenosis
Salman *et al.* [20]	2022	SST k-ω	Non-Newtonian	Both
Bouteloup *et al.* [21]	2020	k-ε	Newtonian	Yes
Nagargoje *et al.* [22]	2020	Laminar	Newtonian	No
Lopes *et al.* [23]	2019	Laminar	Newtonian	No
Sia *et al.* [24]	219	Laminar	Newtonian	Yes
Lee *et al.* [25]	2019	Laminar	Both	No
Azar *et al.* [26]	2019	Laminar	Non-Newtonian	Yes
Yao *et al* [27]	2019	Laminar	Newtonian	No
Kumar *et al.* [28]	2019	Laminar	Both	Yes
Li *et al.* [29]	2019	Laminar	Newtonian	Both
Guerciotti and Vergara [30]	2018	Laminar	Both	Yes
Domanin *et al.* [31]	2018	Laminar	Newtonian	No
Urevc *et al.* [32]	2017	Laminar	Both	No
Bit *et al.* [33]	2017	Laminar	Both	Both
Conti *et al.* [34]	2016	Laminar	Newtonian	Both
Gallo *et al.* [35]	2016	Laminar	Newtonian	No
Sousa *et al.* [36]	2016	Laminar	Newtonian	Both
Gharahi *et al.* [37]	2016	Laminar	Both	Both
Guerciotti *et al.* [38]	2016	Laminar	Newtonian	Both

The assumption is that blood is a non-Newtonian fluid. With the user-defined function for pulsatile blood flow, two non-Newtonian models, Carreau and Cross models, are used. The different parameters like – wall shear stress, velocity distribution, pressure-gradient, etc. are analyzed afterward.

The following are the primary aims of this study:

- To get an idea of how blood flows in different degrees of stenosed arteries.
- To study the non-Newtonian assumption of blood's rheological behavior.
- To analyze the flow characteristics like - wall shear stress, velocity distribution, and pressure distribution in 30% and 70% stenosed arterial geometries.

2 Methodology

This study assumes blood is incompressible and homogenous, and blood flow is non-Newtonian in nature. Besides, the arterial wall is assumed as rigid to avoid complexity though it is naturally elastic in real scenarios. This assumption is valid because due to atherosclerosis, the wall becomes less elastic and more rigid.

The boundary condition employed is based on data from pertinent prior research utilizing Ansys Fluent software in order to compare the outcomes and successfully meet the objectives. The techniques for gathering data and interpreting it are carried out in accordance with prior studies originating from the simulation results.

2.1 CAD Modeling

A carotid artery model is generated in SolidWorks 2020 based on individualized computed tomography (CT) scans of patients. The diameter of exit 1, the internal carotid artery (ICA), is 0.0043 m. The external carotid artery (ECA), or outlet 2, has a diameter of 0.0031 m. Furthermore, the inlet common carotid artery has a diameter of 0.0063 mm. This artery is stenosed at different degrees using SolidWorks 2020 and its flow properties are analyzed. Fig. 5 shows the carotid artery CAD model.

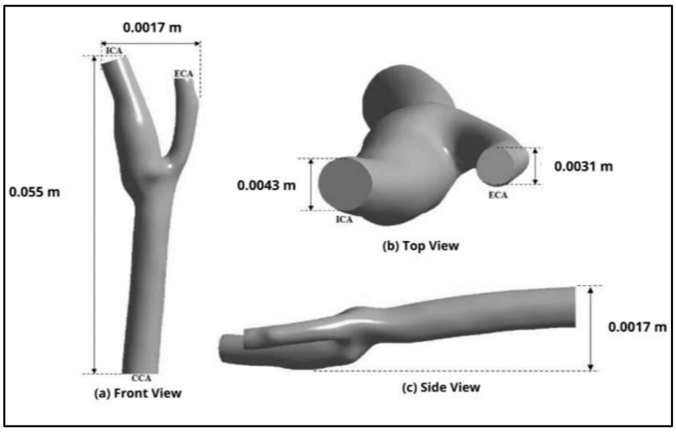

Fig. 5 Carotid Artery CAD Model

2.2 Healthy Carotid Artery Meshing

Meshing is one of the most important parts of a CFD simulation. The precision of outcomes relies on the quantity of elements and nodes employed in the analysis. Computational time will increase if the elements and nodes number is excessively high. So, it is important to follow a proper mesh technique. Fig. 6 illustrates the discretization of the carotid artery's geometry. The number of elements and nodes were 83732 and 27450 respectively where the element size was 1mm. The inflation layer used is of the 'smooth transition' type.

2.3 Governing Equations

The research necessitates fundamental fluid flow equations such as the continuity equation as well as Navier-Stokes, despite the flow complexity.

2.3.1 Continuity Equation

The following is the general continuity equation for fluid flow:

$$\frac{\partial \rho}{\partial t} + \nabla . (\rho v) = 0 \tag{1}$$

Since blood is incompressible, its rate of density change is zero. So, the following will be the modified continuity equation for blood flow:

$$\nabla . (v) = 0 \tag{2}$$

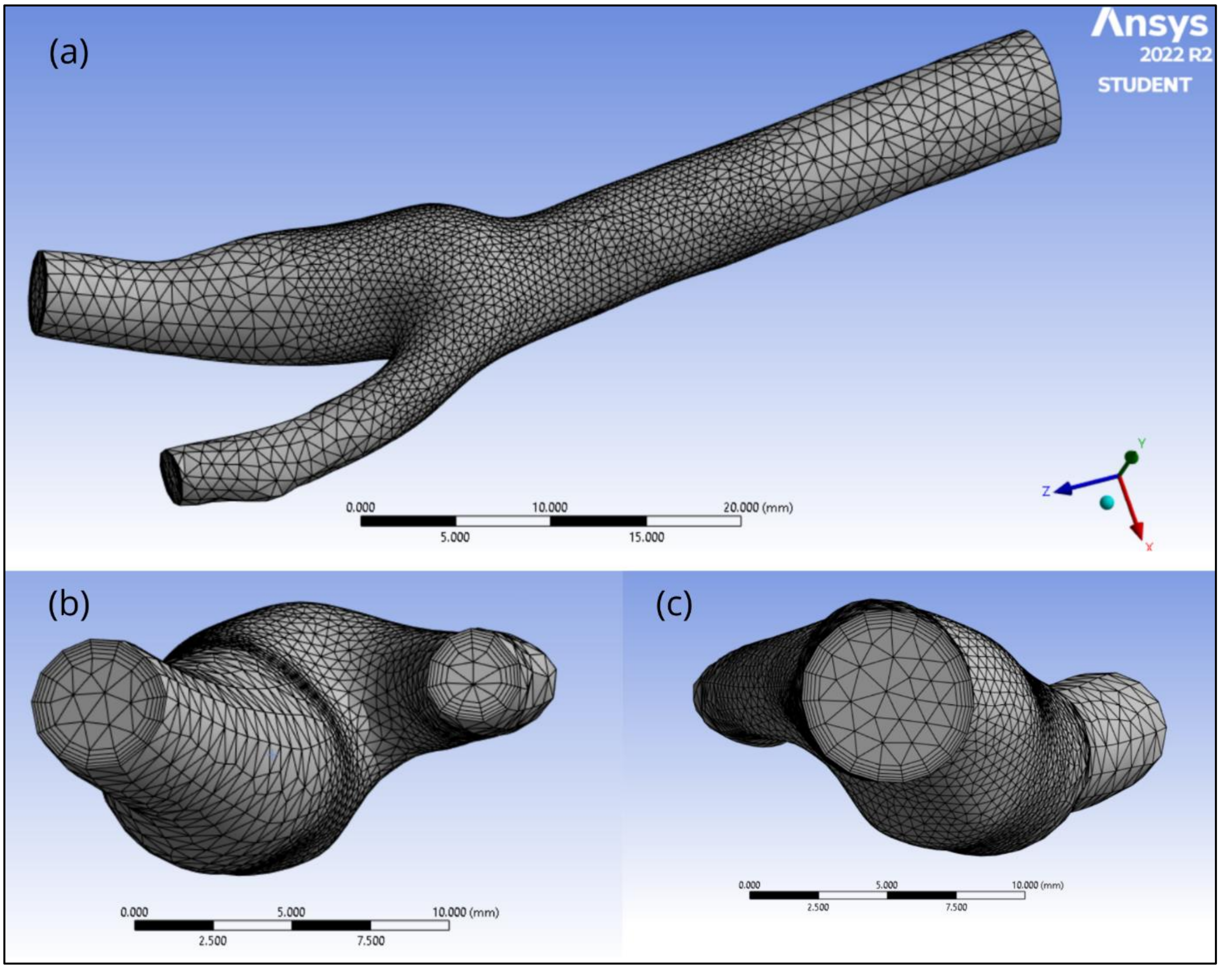

Fig. 6 (a) Meshed representation of a normal carotid artery, (b) Boundary layer at outlets, and (c) Boundary layer at the inlet.

2.3.2 Navier-Stokes Equation

The following is the Navier-Stokes equation for fluid flow:

$$\rho\left(\frac{dv}{dt}+v.(\nabla\, v)\right)=-\nabla\, p+\,\mu\,\nabla^2 v+f \tag{3}$$

In the Eq. (3) provided, the viscosity coefficient varies with shear rate. Consequently, non-Newtonian viscosity models are essential for calculating these viscosity values.

2.4 Viscosity Model

Consideration of viscosity is critical in studying fluid flow, which includes liquids, semi-solids, gases, and solids. Professionals working in the analysis of flow, quality control, research and development, etc. will come across a variety of viscosity measurement methods. Power law, Carreau, Ballyk (or generalized power law), Cross-model, and other non-Newtonian flow viscosity measurement models are examples.

The following is the equation of a Carreau model:

$$\mu_{eff}(\dot{\gamma})=\,\mu_\infty+(\mu_0-\,\mu_\infty)(1+(\lambda\dot{\gamma})^2)^{\frac{n-1}{2}} \tag{4}$$

In Eq. (4) provided, μ_{eff} represents the effective viscosity. μ_0 , μ_{inf} , n, and λ are material coefficients. For blood, Zero-shear viscosity, μ_0 = 0.056 (kg/m.s); Infinite-shear viscosity, μ_∞ = 0.0035 (kg/m.s); Time constant, λ = 3.313 (s); Power law index, n = 0.3568 [39].

The following is the equation of Cross viscosity-model:

$$\mu=\,\mu_\infty+\frac{(\mu_0-\,\mu_\infty)}{1+(\lambda\dot{\gamma})^n} \tag{5}$$

In Eq. (5) above, μ_∞, μ_0, λ, and n are constants. For blood, Zero-shear viscosity, μ_0 = 0.056 (kg/m.s); Infinite-shear viscosity, μ_∞ = 0.0035 (kg/m.s); Time constant, λ = 1.007 (s); Power law index, n = 1.028 [15]. Here, n < 1 symbolizes pseudoplastic fluid, n > 1 is attributed to dilatant fluid, while n=1 means Newtonian fluid.

Fig. 7 shows how viscosity varies with shear rate in the case of non-Newtonian flow.

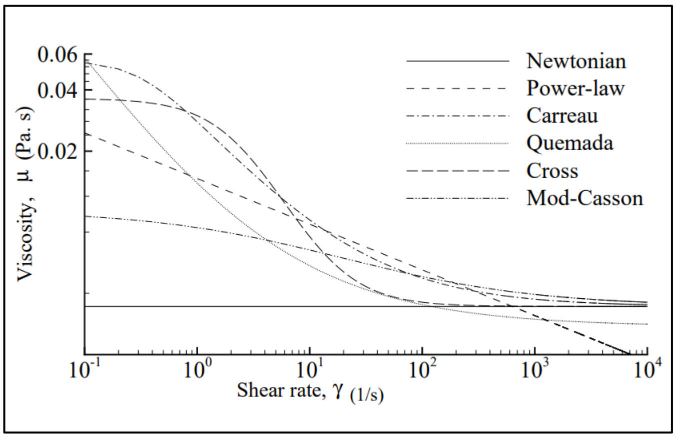

Fig. 7 Relationship between viscosity and shear rate in Newtonian and various non-Newtonian models [40]

2.5 Boundary Conditions

A boundary condition of "no slip" is said to exist along the arterial wall. Consequently, there is no velocity near the wall. The inlet velocity is considered to be pulsatile in nature which varies with time periodically. The model for the pulsatile flow of blood is proposed by Sinnott *et al.* [41]. The inlet velocity profile between two periods, each period having a duration of 0.5s is as the Fig. 8.

The average of a healthy person's pressure when the heart beats (120 mmHg) and pressure when the heart rests (80 mmHg) is 100 mmHg, or 13332 Pascal. This is taken to be the static gauge pressure at the outlets. The following equation is a clear representation of the pulsatile flow inlet velocity:

$$v_{inlet}(t) = \begin{cases} 0.5\, sin[4\pi\,(t + 0.0160236)] : 0.5n < x \ \leq 0.5n + 0.218 \\ 0.1 : 0.5n + 0.218 < n \ \leq 0.5(n+1) \end{cases} \quad (6)$$

where, n = 0, 1, 2 …

2.6 Arterial Model with Stenosis

Fig. 9 represents a sample of the stenosed arteries that is used for analysis. Two samples are taken for consideration, one is 70% stenotic and another is 30% stenotic by dimensions. The number of mesh elements and nodes in the 30% stenotic artery mesh model were 84642 and 27795 respectively, whereas for the 70% stenotic artery, the numbers were 82832 and 27790 respectively. The element size was 1 mm.

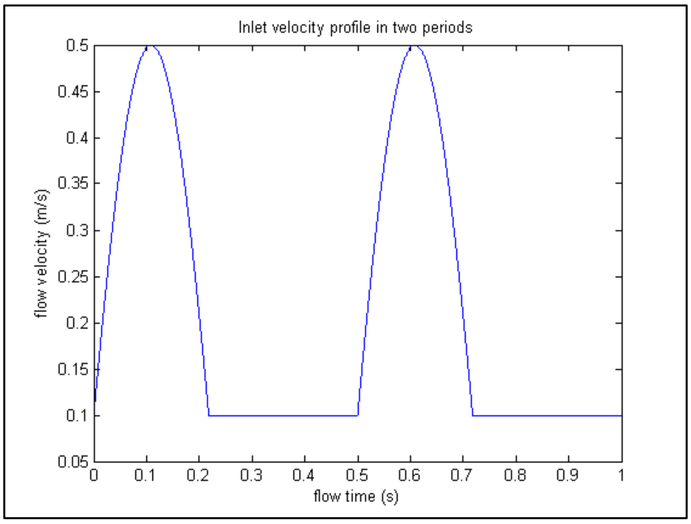

Fig. 8 Inlet velocity profile for pulsatile blood flow

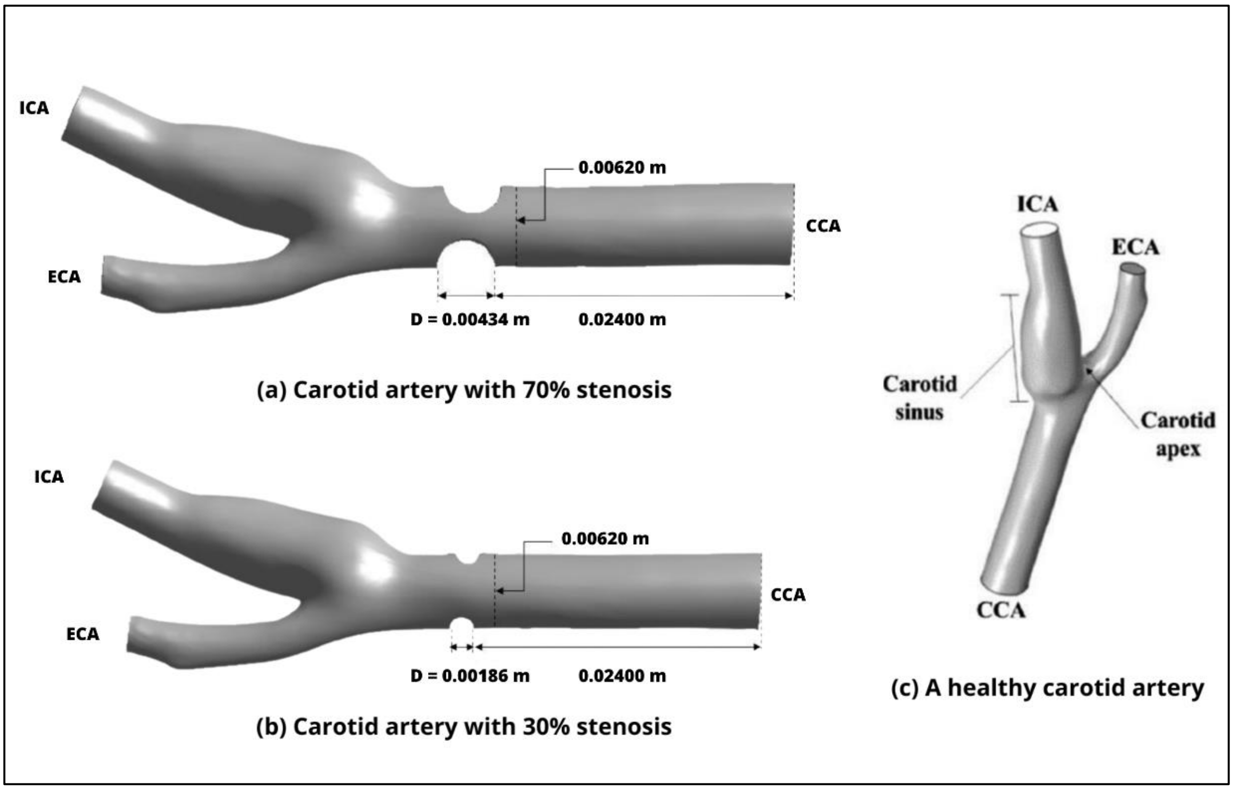

Fig. 9 Model of the carotid artery displaying (a) 70% narrowing, (b) 30% narrowing, and (c) healthy state

2.6.1 30% Stenotic Model Meshing

The generated mesh of the mild stenotic artery, that is, 30% stenotic artery is shown in the Fig. 10.

2.6.2 70% Stenotic Model Meshing

The generated mesh of the moderate stenotic artery, that is, 70% stenotic artery is shown in Fig. 11.

3 Data Collection and Analysis:

The finite volume method (FVM) and pressure-based solver are used for data collecting and computations. The pressure contours, velocity vectors, velocity streamlines and wall shear stress contours are generated over the arterial geometry for both Carreau and Cross model consideration of blood's viscosity.

3.1 Effect of Arterial Stenosis on the Pressure of a Flow Field

The pressure distributions in a healthy carotid artery, 30% stenosed artery, and 70% stenosed artery are demonstrated in Fig. 12-Fig. 14 respectively keeping the time fixed across all the geometries and considering the Carreau viscosity model. In the figures, it is seen that the pressure distribution across a healthy artery is almost the same at all locations. The value is 13332 Pascal which is the mean of the systolic and diastolic pressure of blood in a healthy human artery.

The maximum pressures found in both 30% and 70% stenotic artery are in inlets. The value is found 13386.5 Pa in 30% stenotic artery whereas it is 13419.7 Pa in 70% stenotic artery. In the 30% stenotic artery, the pre-stenotic pressure is about 13357 Pa, and the post-stenotic pressure is about 13356.8 Pa as seen in Fig. 13 with the help of variable probing. The pressure value at the stenosis region is 13332.3 Pa and bifurcating region is 13368.3 Pa. Besides, in 70% stenotic artery in Fig. 14, the pre-stenotic pressure is about 13399 Pa whereas the post-stenotic pressure is about 13344.4 Pa. The pressure at the stenotic region is 13353.2 Pa and at a bifurcation is 13368.9 Pa. Again, the pressure distributions in a healthy artery, 30% stenosed artery, and 70% stenosed artery are shown in Fig. 15-Fig. 17 respectively keeping the time fixed across all the geometries and considering the Cross viscosity-model. In Fig. 15, it is seen that the inlet possesses the maximum pressure whereas outlets possess the minimum. The pressure ranges from 13332 Pa to 13549.446 Pa. The decrease of pressure is almost uniform in a healthy carotid artery.

The maximum pressures found in both 30% and 70% stenotic artery are in inlets. The value is found 14256.2 Pa in 30% stenotic artery whereas it is 14478.4 Pa in 70% stenotic artery. In the 30% stenotic artery, the pre-stenotic pressure is about 13863.1 Pa, and the post-stenotic pressure is about 13780.1 Pa as seen in Fig. 16. Besides, the stenotic region's pressure is 13809.7 Pa and bifurcating region is 14238 Pa. Besides, in 70% stenotic artery as seen in Fig. 17, the pre-stenotic pressure is about 14095 Pa whereas the post-stenotic pressure is about 13732 Pa. The pressure at the stenotic region is 13915.6 Pa and at bifurcation is 14478.4 Pa. The pressure decline from the pre-stenotic region to the post-stenotic region is greater in 70% stenosis than in 30% stenosis using both viscosity models. This pressure difference may push blood with greater speed and cause fatal consequences to patients with high blood pressure.

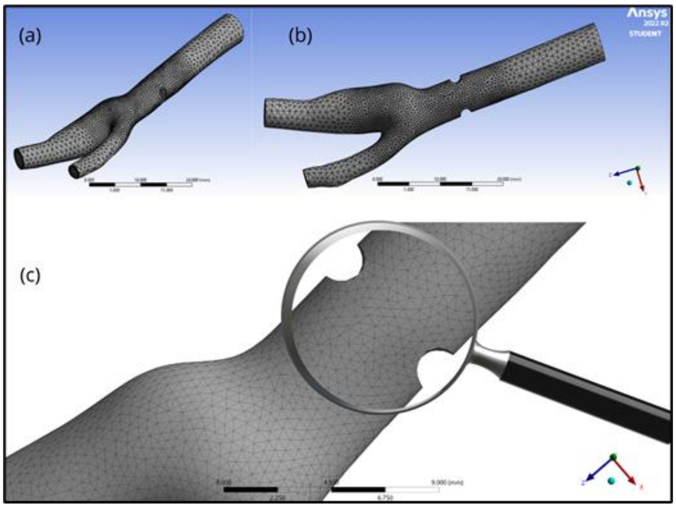

Fig. 10 Meshed representation of a 30% narrowed artery model, shown in (a) isometric view, (b) top view, and (c) magnified view of the stenosis area

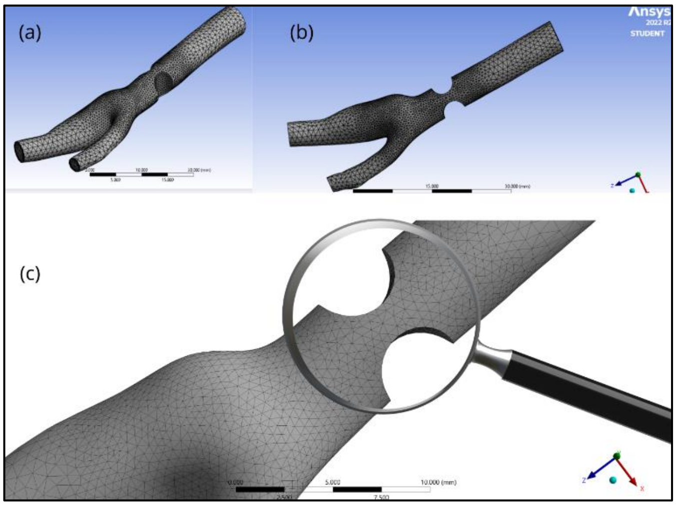

Fig. 11 Meshed representation of a 70% narrowed artery model, shown in (a) isometric view, (b) top view, and (c) magnified view of the stenosis area

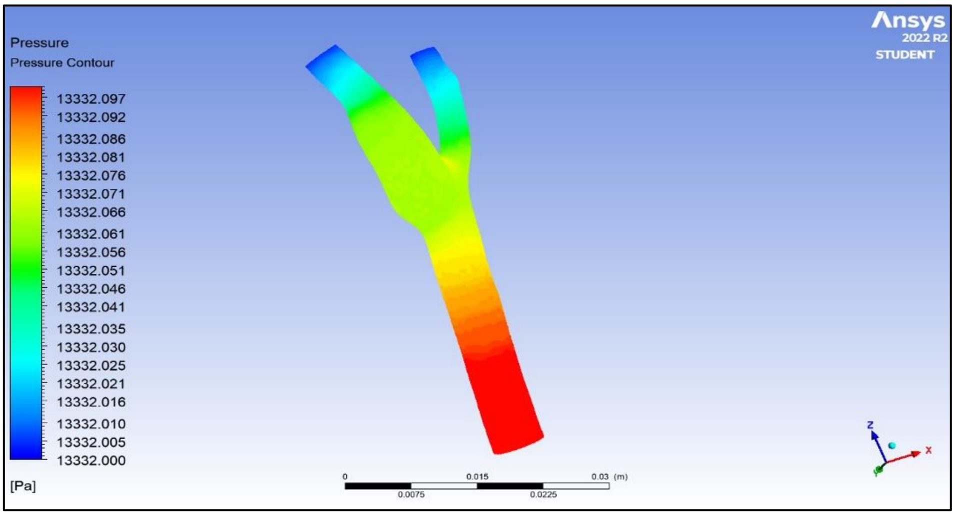

Fig. 12 Pressure contour of a healthy carotid artery (Carreau Viscosity Model)

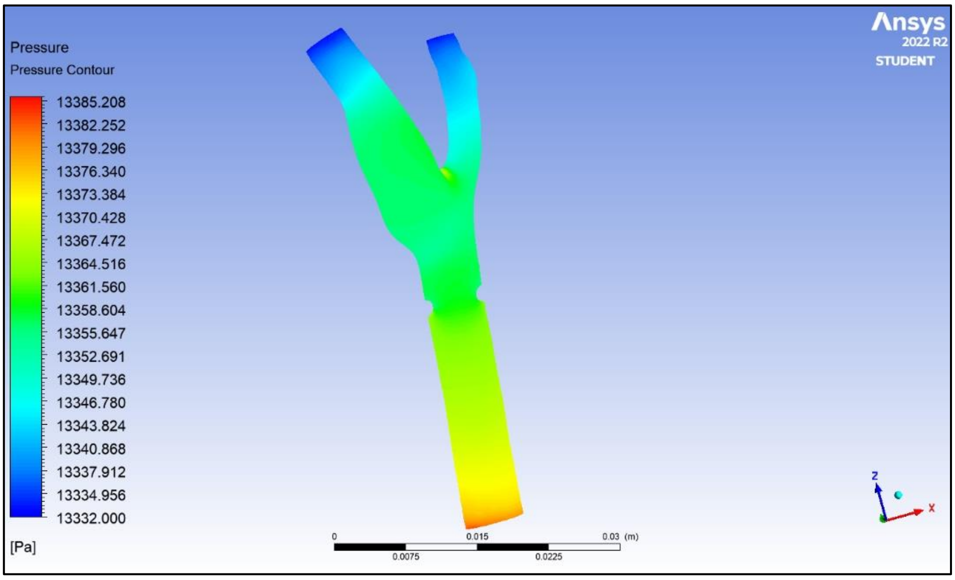

Fig. 13 Pressure contour of a 30% stenosed carotid artery (Carreau Viscosity Model)

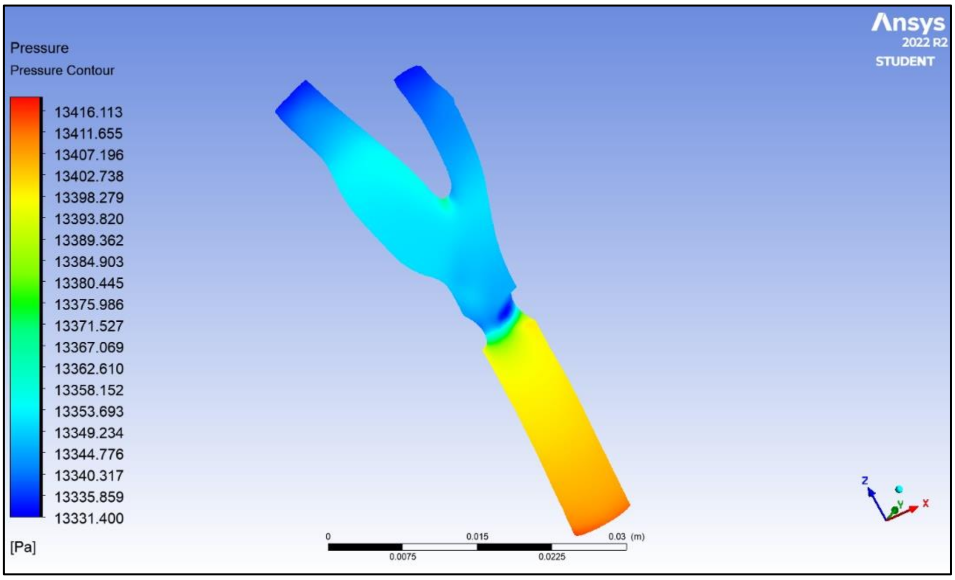

Fig. 14 Pressure contour of a 70% stenosed carotid artery (Carreau Viscosity Model)

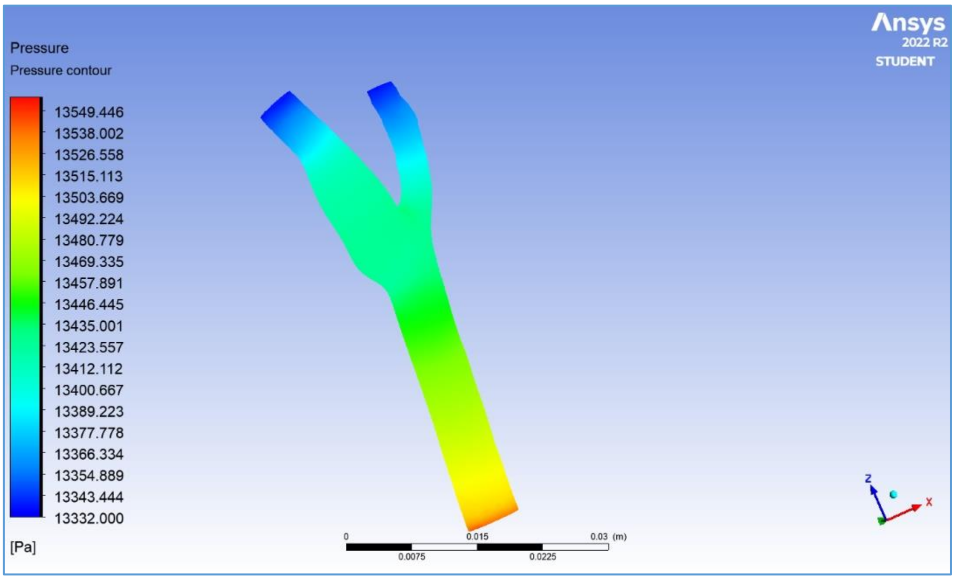

Fig. 15 Pressure contour of a healthy carotid artery (Cross Viscosity Model)

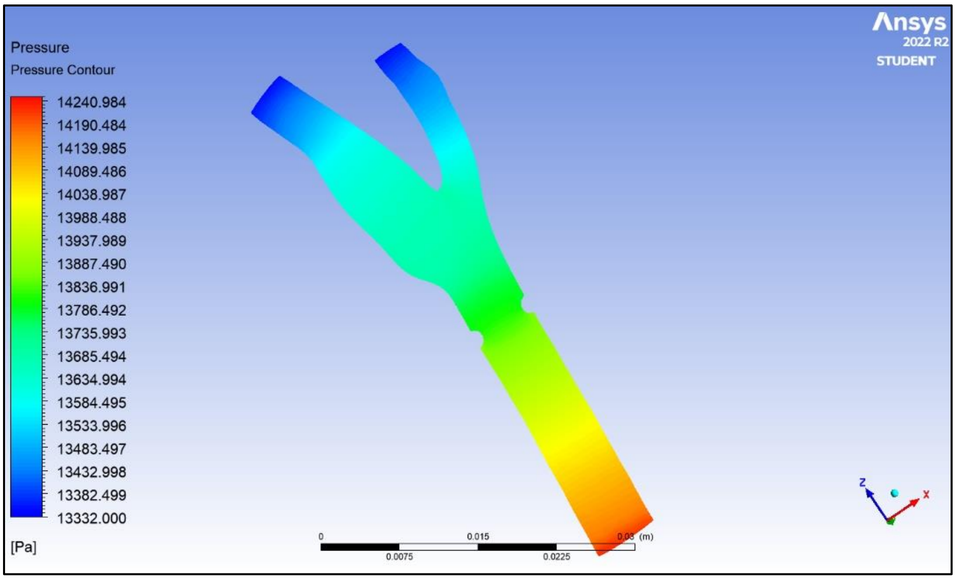

Fig. 16 Pressure contour of a 30% stenosed carotid artery (Cross Viscosity Model)

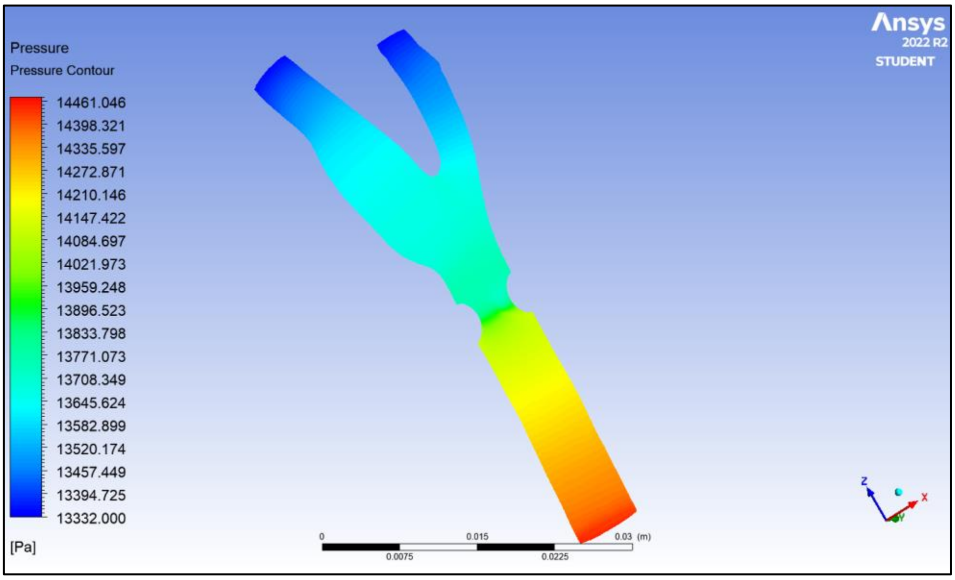

Fig. 17 Pressure contour of a 70% stenosed carotid artery (Cross Viscosity Model)

3.2 Effect of Arterial Stenosis on the Velocity of a Flow Field

The velocity distribution in a healthy carotid artery, 30% stenosed artery, and 70% stenosed artery are shown in Fig. 18-Fig. 20 respectively keeping the time fixed across all the geometries and considering the Carreau viscosity model. The inlet velocity in all the cases begins with the same magnitude.

In the healthy artery, the velocity increases in a uniform fashion as seen in Fig. 18. The maximum velocity found in 30% stenotic artery is in outlet 1 whereas 70% stenotic artery has a maximum velocity at the stenotic region. The value is found 0.228616 m/s in 30% stenotic artery whereas it is 0.373931 m/s in 70% stenotic artery. In the 30% stenotic artery, the pre-stenotic velocity is about 0.0341079 m/s and the post-stenotic velocity is about 0.0572985 m/s as seen in Fig. 19. The average velocity at the 30% stenosis region is 0.108183 m/s. Besides, in 70% stenotic artery, the pre-stenotic velocity is about 0.15031 m/s whereas the post-stenotic velocity is about 0.328816 m/s as seen in Fig. 20.

Again, the velocity distributions in a healthy artery, 30% stenosed artery, and 70% stenosed artery are shown in Fig. 21-Fig. 23 respectively keeping the time fixed across all the geometries and considering the Cross viscosity-model. In Fig. 21, it is seen that a healthy artery has almost a uniform velocity distribution across the geometry. The velocity magnitude ranges from 0 m/s at the walls to 0.283 m/s at the center of the outlet 1. The maximum velocity found in 30% stenotic artery is in outlet 1 whereas 70% stenotic artery has a maximum velocity at the stenotic region. The value is found 0.365995 m/s in 30% stenotic artery as seen in Fig. 22 whereas it is 0.673342 m/s in 70% stenotic artery as seen in Fig. 23. In 30% stenotic artery, the pre-stenotic velocity is about 0.0035434 m/s and post-stenotic velocity is about 0.00314036 m/s as seen in Fig. 23. The velocity at the 30% stenosis region is 0.0183052 m/s. Besides, in 70% stenotic artery, the pre-stenotic velocity is about 0.00144266 m/s whereas the post-stenotic velocity is about 0.291151 m/s. Out of all the cases, the highest velocity observed is in the 70% stenotic region.

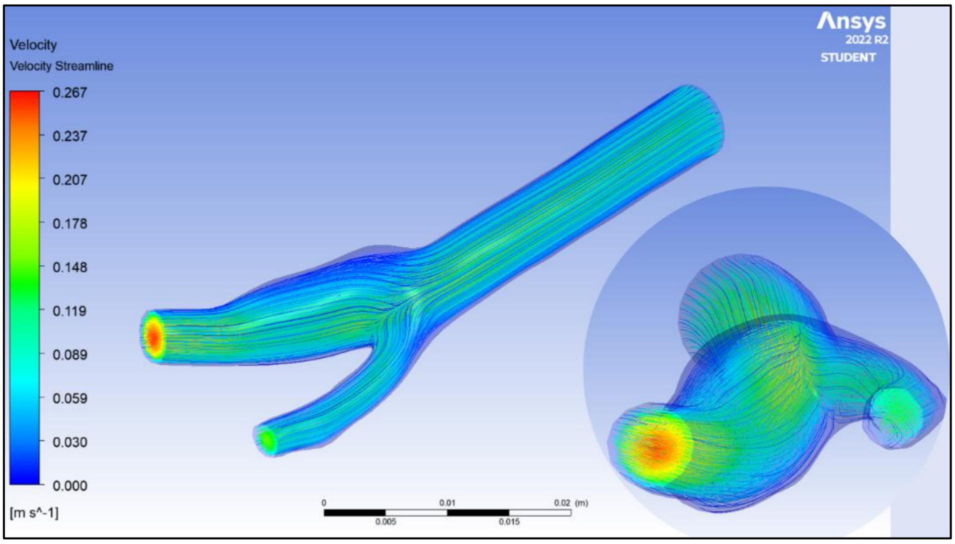

Fig. 18 Velocity streamlines of a healthy artery with its front view considering Carreau model

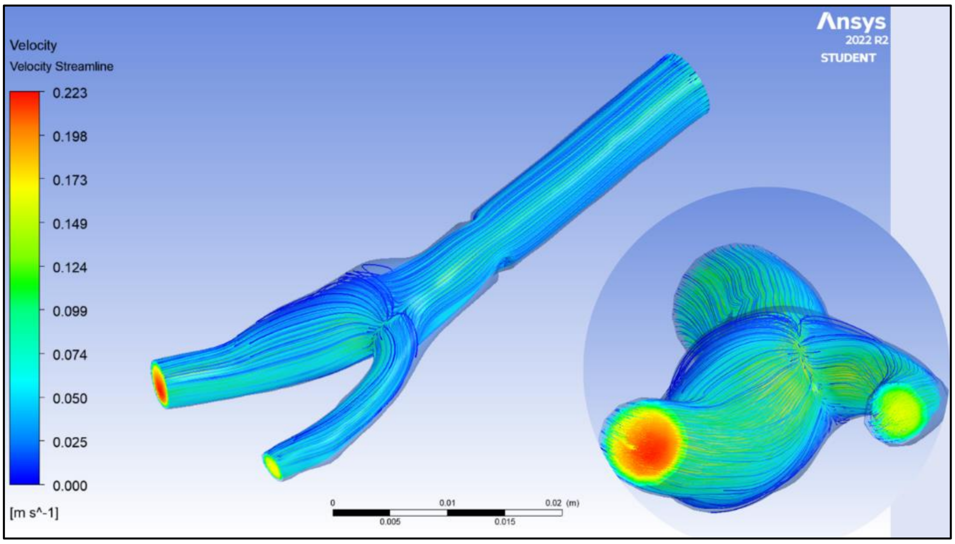

Fig. 19 Velocity streamlines of a 30% stenotic artery with its front view considering Carreau model

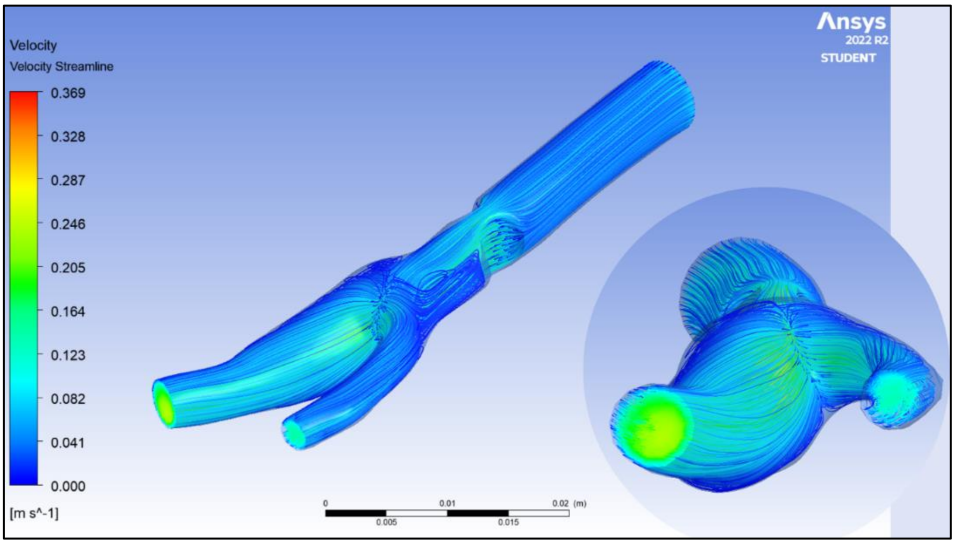

Fig. 20 Velocity streamlines of a 70% stenotic artery with its front view considering Carreau model

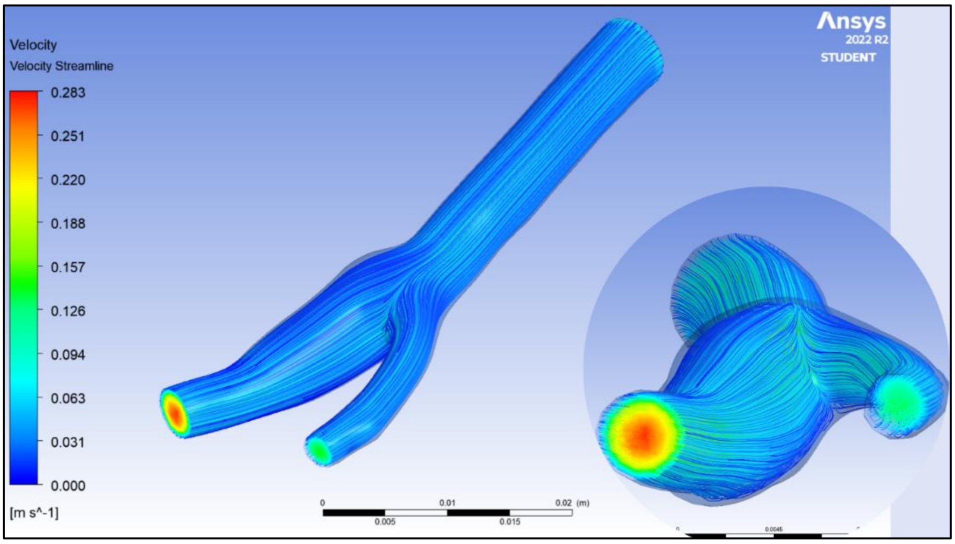

Fig. 21 Velocity streamlines of a healthy artery with its front view considering Cross model

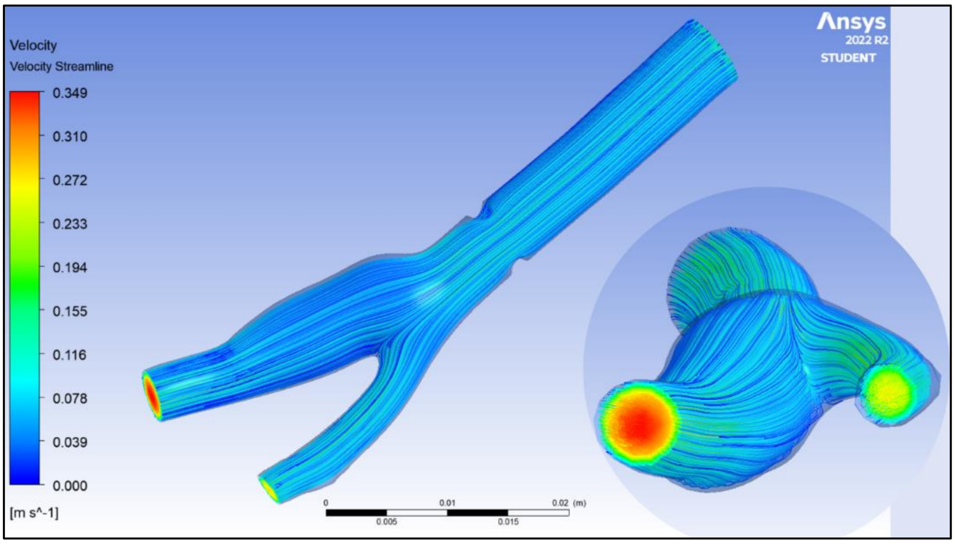

Fig. 22 Velocity streamlines of a 30% stenotic artery with its front view considering Cross model

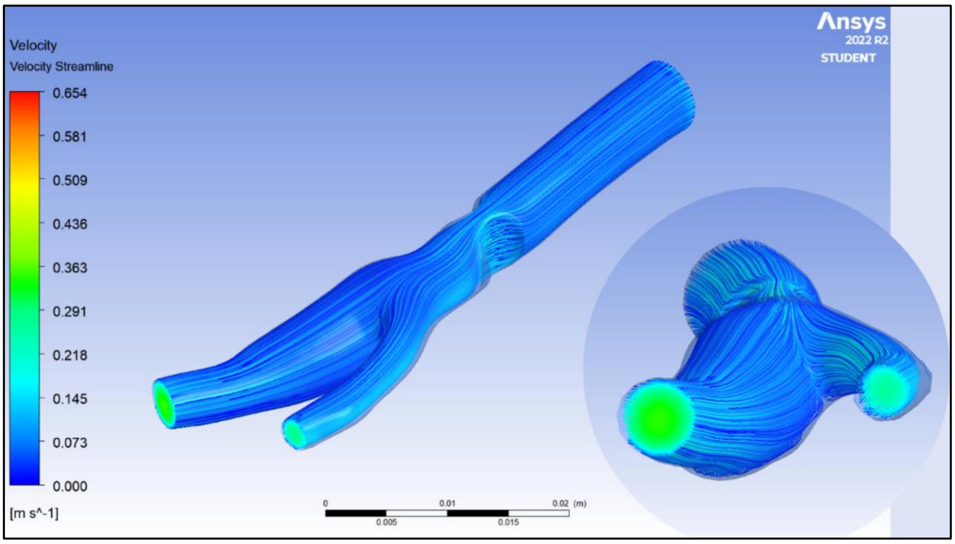

Fig. 23 Velocity streamlines of a 70% stenotic artery with its front view considering Cross model

3.3 Effect of Arterial Stenosis on the Wall Shear Stress

Wall shear stress (WSS) is one of the major determiners of the severity of stenosis. Understanding the severity of vascular stenosis requires knowledge of WSS. High WSS lengthens endothelial cells and forces them to align with the flow direction. Low WSS has little impact on the cell, but it increases intercellular permeability, which in turn accelerates plaque formation. Therefore, WSS is one of the reasons for developing a new stenosis throat. Wall shear stress depends on the viscosity as well as the velocity gradient of the fluid flow. In Fig. 24-Fig. 26, the wall shear stress is shown for Carreau model of blood's viscosity for a healthy artery, 30% stenotic artery, and 70% stenotic artery respectively. From the figures, it is observed that the shear stress in a healthy arterial wall is almost uniform as seen in Fig. 24. But in a 30% stenotic artery in Fig. 25, shear stress is the highest in the bifurcating region and it is slightly lower in the stenotic throat. However, in the case of 70% stenosis in Fig. 26, it is observed that the stenotic region has the maximum wall shear stress value. Its value in the bifurcating region is slightly lower. In Fig. 27-Fig. 29, the wall shear stress is shown for the Cross model of blood's viscosity for a healthy artery, 30% stenotic artery, and 70% stenotic artery respectively. The values of the wall shear stress observed using the Cross model are greater than the Carreau model in all three geometries of healthy artery, 30% stenotic artery, and 70% stenotic artery. However, the contour of a healthy artery is almost similar in both cases. In Fig. 28, the wall shear stress of a 30% stenotic artery is observed. Here the stenosis region has the maximum value and the value at the bifurcating region is lower. The rest of the geometry has an average wall stress value. In Fig. 29, the wall shear stress of a 70% stenotic artery is exhibited. This contour is similar to the contour of the Carreau model as the maximum shear stress is observed in the stenosis region. But the value at the bifurcating region is lower. In both cases, the wall shear stress is maximum at the stenotic region for 30% and 70% stenosis respectively.

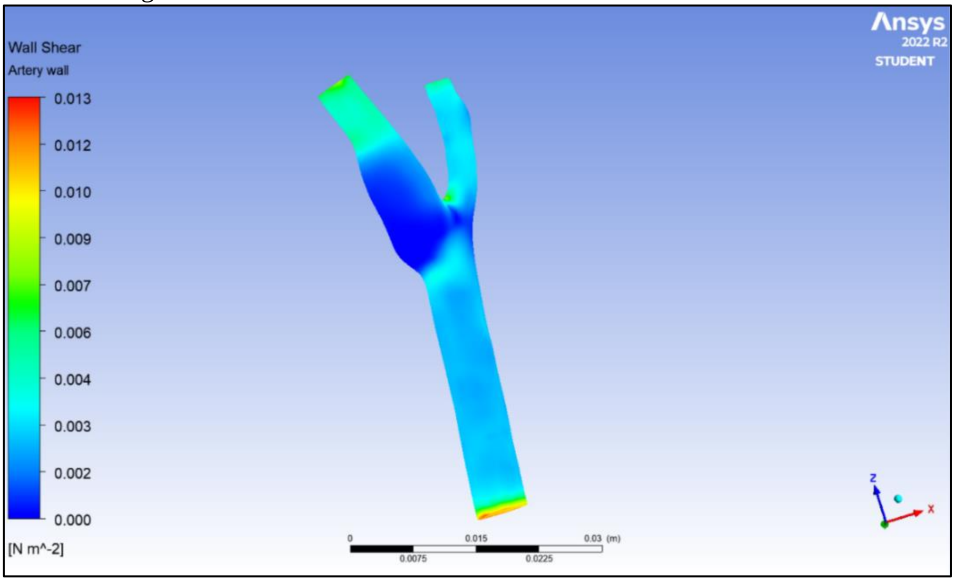

Fig. 24 Wall shear stress of a healthy artery considering Carreau model

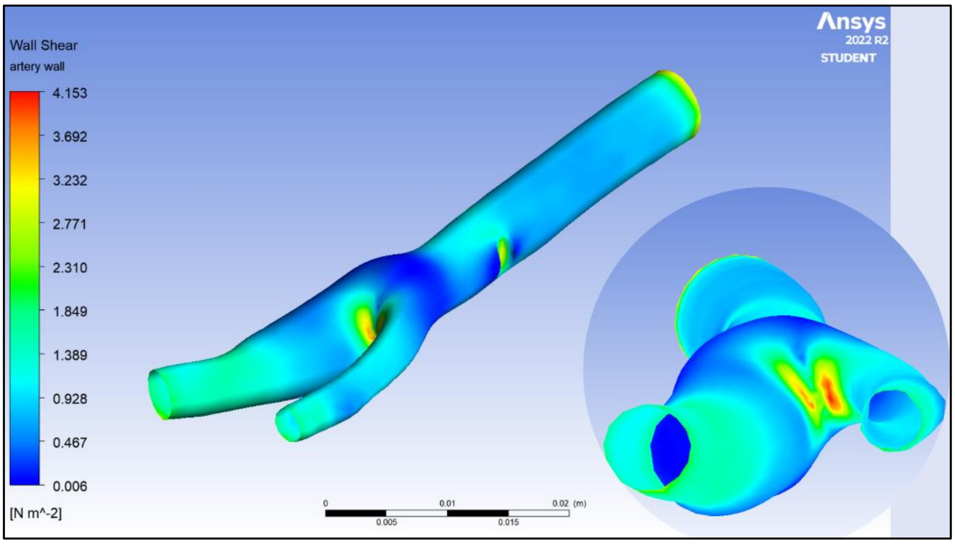

Fig. 25 Wall shear stress of a 30% stenotic artery with its front view considering Carreau model

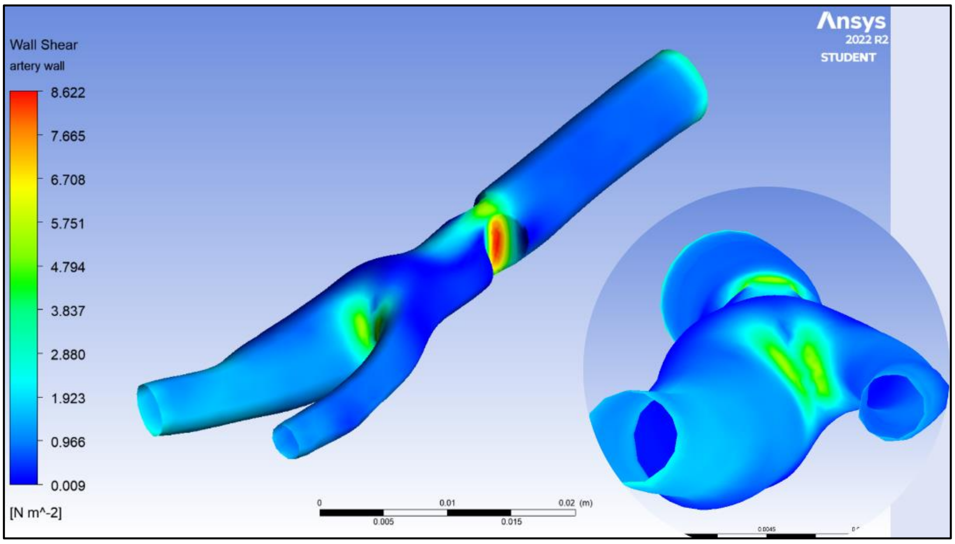

Fig. 26 Wall shear stress of a 70% stenotic artery with its front view considering Carreau model

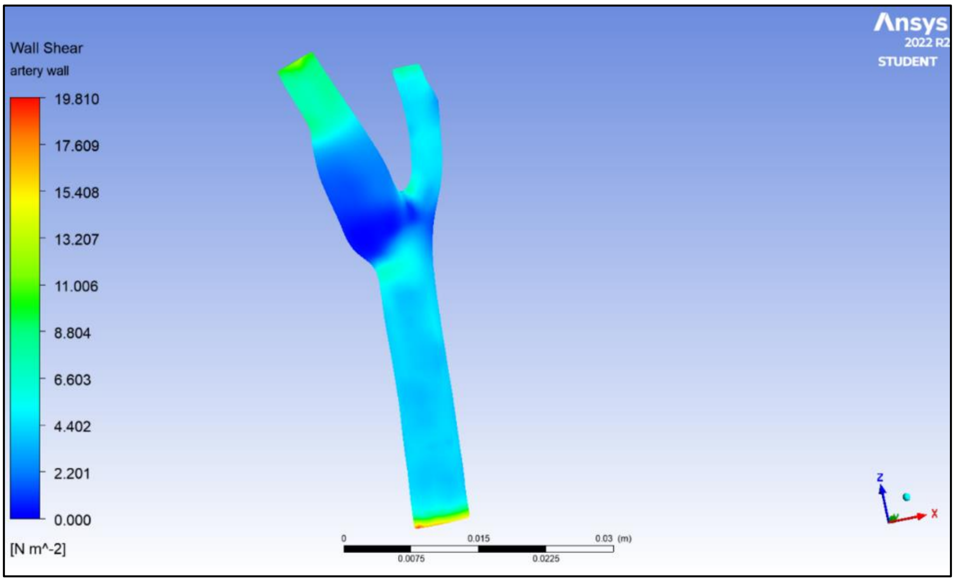

Fig. 27 Wall shear stress of a healthy artery considering Cross model

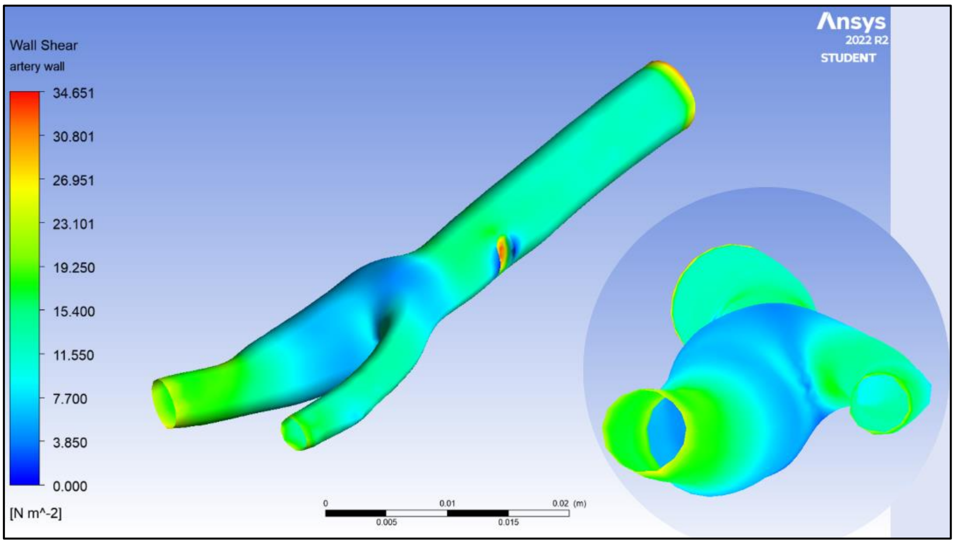

Fig. 28 Wall shear stress of a 30% stenotic artery with its front view considering Cross model

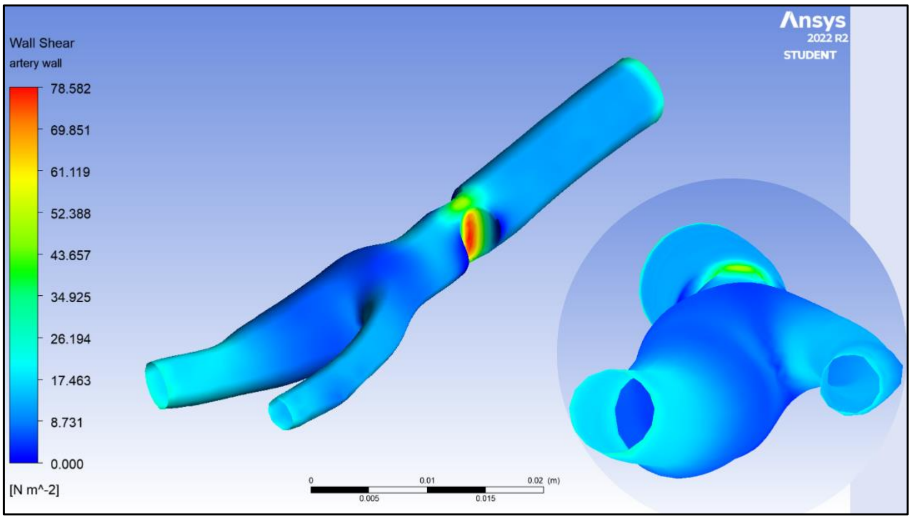

Fig. 29 Wall shear stress of a 70% stenotic artery with its front view considering Cross model

4 Results and Discussion

The results generated in the study are discussed in brief. The results are of total pressure, velocity magnitude, and wall shear stress considering Carreau and Cross model of blood's viscosity.

4.1 Results

The study focused on finding the total pressure, velocity magnitude, and wall shear stress for both Carreau and Cross model. The results help to compare the two different models. The coordinates of the center line taken for the purpose of graphically representing the results ranged from (0.003079758, 0.006003463, -0.03183488) to (0.003080636, 0.003186158, -0.000693613). The line has been shown in Fig. 30. The line extends from the inlet region, and includes the pre-stenotic region to the post-stenotic region. It terminates just at the pre-bifurcation region of the carotid artery. The properties along this line will represent the actual blood flow properties. In Fig. 31 below, the comparison of total pressure value is shown for both the models, Carreau and Cross, and all three geometries, that is healthy, 30% stenotic, and 70% stenotic artery. The area within the red dots in the figure represents the 70% stenotic region and the area within the green dots represents the 30% stenotic region. From Fig. 31, it is seen that the 70% stenotic artery with Cross model consideration has the highest pressure decline amongst all the other geometries. The pressure values converge to a point at the post-statistic region in the Cross-model consideration. This is not the same in the case of Carreau-model consideration. In the Carreau model, a slight pressure decline occurs in the 70% stenotic artery. However, the pressure at the healthy artery and 30% stenotic artery is almost uniform throughout all the positions of the considered line. In Fig. 32, the comparison of velocity magnitude is shown for both the models, Carreau and Cross, and for all three geometries, that is healthy, 30% stenotic and 70% stenotic artery. The area within the red dots in the figure represents the 70% stenotic region and the area within the green dots represents the 30% stenotic region. From Fig. 32, it is seen that the 70% stenotic artery with Cross model consideration has the highest velocity amongst all the other geometries. The Carreau model with 70% stenosis has the second highest value. The velocity values converge to a point at a position of 0.027m where the velocity for both the models is 0.3 m/s. Apart from the 70% stenotic artery, all the other geometries follow a uniform rise in velocity across the line. The healthy artery and the 30% stenotic artery have almost the same velocity throughout the line except in the stenotic region. Table 2 and Table 3 below depict the maximum and minimum values of pressure and velocity distribution within the line under consideration. The results obtained from the simulated data are illustrated in Table 4 and Table 5.

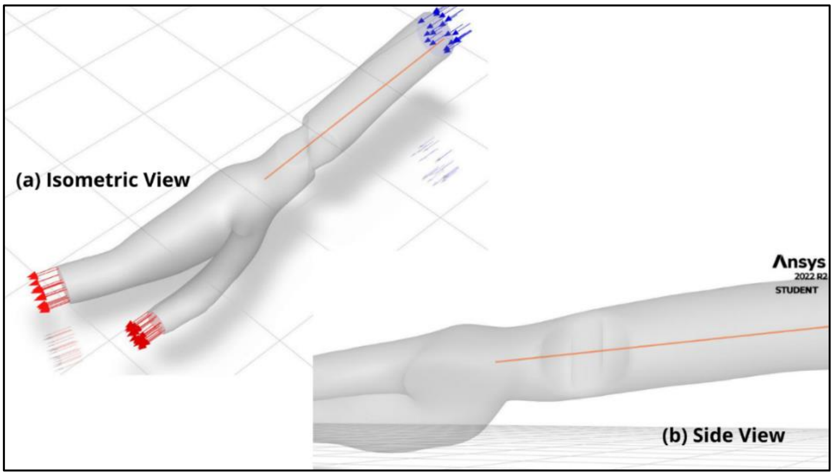

Fig. 30 A center-line for analysis

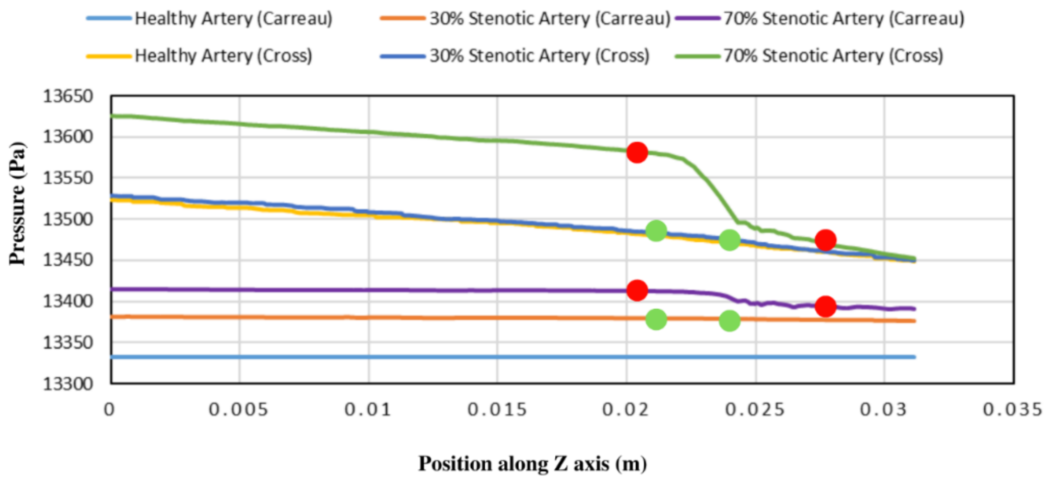

Fig. 31 Comparative analysis of total pressure for Carreau and Cross model

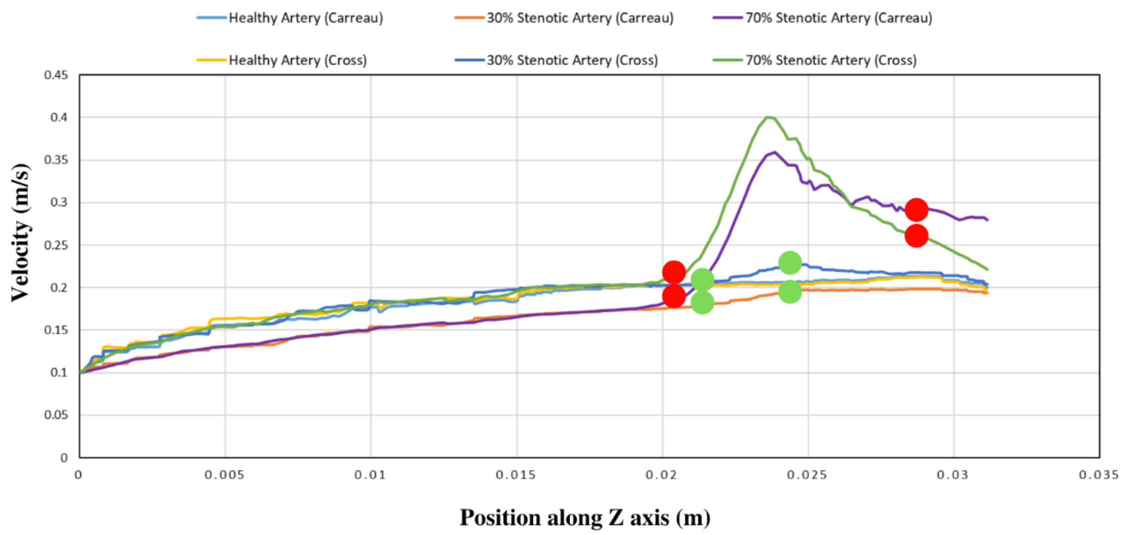

Fig. 32 Comparative analysis of velocity magnitude for Carreau and Cross model

Table 2 Numerical results of Carreau and Cross model for pressure distribution along the line

	Healthy (Carreau)	30% Stenotic (Carreau)	70% Stenotic (Carreau)	Healthy (Cross)	30% Stenotic (Cross)	70% Stenotic (Cross)
Maximum Pressure (Pa)	13332.1	13382	13415.3	13523.5	13528	13625.1
Minimum Pressure (Pa)	13332.1	13375.6	13391	13448	13450.2	13452.7

Table 3 Numerical results of Carreau and Cross model for velocity distribution along the line

	Healthy (Carreau)	30% Stenotic (Carreau)	70% Stenotic (Carreau)	Healthy (Cross)	30% Stenotic (Cross)	70% Stenotic (Cross)
Maximum Velocity (m/s)	0.213396	0.198765	0.358833	0.212879	0.22738	0.400163
Minimum Velocity (m/s)	0.100253	0.100104	0.100131	0.100313	0.100313	0.100316

Table 4 Numerical results of Carreau Model for the entire geometry

Carreau Viscosity Model Values				
	30% Stenotic Artery		70% Stenotic Artery	
	Maximum	Minimum	Maximum	Minimum
Pressure (Pa)	13386.5 (Inlet)	13332 (Outlets)	13419.7 (Inlet)	13332 (Oulets)
Wall Shear Stress (Nm^{-2})	4.57917 (Bifurcating region)	0.00746572 (Post-stenotic region)	9.17718 (Stenotic region)	0.183745 (Post-stenotic region)
Velocity (ms^{-1})	0.228616 (Outlet 1)	0 (Artery wall no slip)	0.373931 (Stenotic region)	0 (Artery wall no slip)

Table 5 Numerical results of Cross Model for the entire geometry

Cross Viscosity Model Values				
	30% Stenotic Artery		70% Stenotic Artery	
	Maximum	Minimum	Maximum	Minimum
Pressure (Pa)	14256.2 (Inlet)	13332 (Outlets)	14478.4 (Inlet)	13332 (Outlets)
Wall Shear Stress (Nm^{-2})	39.7529 (Stenotic region)	3.28711 (Post-stenotic region)	83.3195 (Stenotic region)	0.0295918 (Post-stenotic region)
Velocity (ms^{-1})	0.365995 (Outlet 1)	0 (Artery wall no slip)	0.673342 (Stenotic region)	0 (Artery wall no slip)

4.2 Discussion

The results obtained from simulated data and graphs indicate that with the increase of stenosis from mild to moderate, that is from 30% stenotic artery to 70% stenotic artery, the rheological properties of blood vary. For Carreau model consideration, the pressure is decreased by 0.41% from the inlet to the outlets in a 30% stenotic artery. Again, in the 70% stenotic artery, the value has decreased by 0.65% from the inlet to the outlets. For Cross model consideration, the 30% stenotic artery shows a decline of 6.48% in pressure while the 70% stenotic artery shows a 7.92% decline from the inlet to the outlets of the carotid artery. Furthermore, the wall shear stress ranges from 0.00746572 N/m^2 to 4.5917 N/m^2 in a 30% stenotic artery for Carreau model consideration. For 70% stenotic artery, this range is from 0.183745 N/m^2 to 9.17718 N/m^2. For Cross model consideration, this range is even larger. Out of all the considerations, the maximum velocity has been observed in 70% stenotic artery at the stenosis region and the value is 0.673342 m/s. The maximum pressure value also has been observed in 70% stenotic artery for the Cross model and the value is 14478.4 Pa. The wall shear stress is also the highest at 70% stenotic artery at the stenosis region and its value is 83.3195 Nm-2.

5 Conclusion and Recommendation

This study on different geometries of carotid artery stenosis can help medical practitioners to provide support through early diagnosis, compare the results, and provide patient-specific treatments. The blood's velocity rise and high inlet pressure, especially in the Cross model, indicate certain areas of an artery that need medical attention. The maximum velocity for 70% stenotic artery was found to be in the stenosis region and so, due to this high velocity, this region is more prone to endothelial damage and plaque formation. The pressure within an artery determines how resistant the flow is in the artery. From the study, it was seen that the stenosis has caused an increase of pressure at the inlets and it gradually decreased downstream, at the post-stenotic region. Alongside that, the values also indicate that there is a proportional relation between pressure and the severity of stenosis. From this information, one can assess the hemodynamic impact of stenosis and make effective treatment decisions. The value of wall shear stress was found to be the maximum at the stenotic region and lower at the region of bifurcation, which indicates a potential site for angioplasty or stenting. Overall, among the two models used for this study, the higher pressure and WSS in Cross model indicate its suitability for severe stenosis representation.

For future studies, blood flow can be considered turbulent, which will resemble more with the actual scenario for stenosis. The elastic nature of arterial geometry can be taken into consideration for analysis as it is more realistic. For the approximation of blood flow, the other non-Newtonian models except the two used in this study can be used for analysis. For example, the Generalized Power Law model or Ballyk model, Casson model, Carreau – Yasuda model, etc.

References

[1] "The top 10 causes of death," World Health Organization, Dec. 09, 2020. https://www.who.int/news-room/fact-sheets/detail/the-top-10-causes-of-death (accessed Sep. 23, 2023).

[2] "Report on Bangladesh Sample Vital Statistics 2018," May 2019. Accessed: Sep. 23, 2023. [Online]. Available: https://bbs.portal.gov.bd/sites/default/files/files/bbs.portal.gov.bd/page/6a40a397_6ef7_48a3_80b3_78b8d1223e3f/SVRS_Report_2018_29-05-2019%28Final%29.pdf

[3] "Heart attacks the most common cause of death in Bangladesh last year: BBS," The Daily Star, Mar. 10, 2021. https://www.thedailystar.net/bangladesh/news/heart-attacks-the-most-common-cause-death-bangladesh-last-year-bbs-2058233 (accessed Sep. 23, 2023).

[4] "Atherosclerosis," Encyclopaedia Britannica, Inc. Apr. 23, 2020. Accessed: Sep. 23, 2023. [Online]. Available: https://www.britannica.com/science/atherosclerosis

[5] "Carotid Stenosis," Temple Health, Jun. 28, 2021. https://www.templehealth.org/services/conditions/carotid-stenosis (accessed Sep. 23, 2023).

[6] Köhler, U., Marshall, I., Robertson, M.B., Long, Q., Xu, X.Y. and Hoskins, P.R., 2001. MRI measurement of wall shear stress vectors in bifurcation models and comparison with CFD predictions. *Journal of Magnetic Resonance Imaging: An Official Journal of the International Society for Magnetic Resonance in Medicine*, 14(5), pp.563-573.

[7] Marshall, I., Zhao, S., Papathanasopoulou, P., Hoskins, P. and Xu, X.Y., 2004. MRI and CFD studies of pulsatile flow in healthy and stenosed carotid bifurcation models. *Journal of Biomechanics*, 37(5), pp.679-687.

[8] Tu, J., Wong, K.K., Cheung, S.C., Beare, R. and Phan, T., 2011. Analysis of patient-specific carotid bifurcation models using computational fluid dynamics. *Journal of Medical Imaging and Health Informatics*, *1*(2), pp.116-125.

[9] Khader, A.S., Shenoy, S.B., Pai, R.B., Kamath, G.S., Sharif, N.M. and Rao, V.R.K., 2011. Effect of increased severity in patient specific stenosis of common carotid artery using CFD—a case

study. *World journal of Modelling and Simulation*, *7*(2), pp.113-122.

[10] Li, M.X., Beech-Brandt, J.J., John, L.R., Hoskins, P.R. and Easson, W.J., 2007. Numerical analysis of pulsatile blood flow and vessel wall mechanics in different degrees of stenoses. *Journal of Biomechanics*, *40*(16), pp.3715-3724.

[11] Chua, C.S., Sheard, G.J., Ryan, K. and Fouras, A., 2008. Changes in flow and wall stresses through arterial constrictions offset from the centre of the vessel. *Anziam Journal*, *50*, pp.C744-C759.

[12] Li, Z.Y., Taviani, V., Tang, T., Sadat, U., Young, V., Patterson, A., Graves, M. and Gillard, J.H., 2009. The mechanical triggers of plaque rupture: shear stress vs pressure gradient. *The British journal of radiology*, *82*(special_issue_1), pp.S39-S45.

[13] Lorenzini, G. and Casalena, E., 2008. CFD analysis of pulsatile blood flow in an atherosclerotic human artery with eccentric plaques. *Journal of Biomechanics*, *41*(9), pp.1862-1870.

[14] Mandal, P.K., 2005. An unsteady analysis of non-Newtonian blood flow through tapered arteries with a stenosis. *International Journal of Non-linear Mechanics*, *40*(1), pp.151-164.

[15] Cho, Y.I. and Kensey, K.R., 1991. Effects of the non-Newtonian viscosity of blood on flows in a diseased arterial vessel. Part 1: Steady flows. *Biorheology*, *28*(3-4), pp.241-262.

[16] Johnston, B.M., Johnston, P.R., Corney, S. and Kilpatrick, D., 2004. Non-Newtonian blood flow in human right coronary arteries: steady state simulations. *Journal of biomechanics*, *37*(5), pp.709-720.

[17] Gijsen, F.J., van de Vosse, F.N. and Janssen, J.D., 1999. The influence of the non-Newtonian properties of blood on the flow in large arteries: steady flow in a carotid bifurcation model. *Journal of biomechanics*, *32*(6), pp.601-608.

[18] Formaggia, L., Lamponi, D. and Quarteroni, A., 2003. One-dimensional models for blood flow in arteries. *Journal of engineering mathematics*, *47*, pp.251-276.

[19] Lee, K.W. and Xu, X.Y., 2002. Modelling of flow and wall behaviour in a mildly stenosed tube. *Medical Engineering & Physics*, *24*(9), pp.575-586.

[20] Ramdan, S.A., Rasani, M.R., Subramaniam, T., Muda, A.S., Aziz, A.F.A., Ya, T.M.Y.S.T., Moria, H., Tahir, M.F.M. and Nuawi, M.Z., 2022. Blood flow acoustics in carotid artery. *Journal of Advanced Research in Fluid Mechanics and Thermal Sciences*, *94*(1), pp.28-44.

[21] Bouteloup, H., de Oliveira Marinho, J.G. and Espino, D.M., 2020. Computational analysis to predict the effect of pre-bifurcation stenosis on the hemodynamics of the internal and external carotid arteries. *Journal of Mechanical Engineering and Sciences*, *14*(3), pp.7029-7039.

[22] Nagargoje, M. and Gupta, R., 2020. Effect of sinus size and position on hemodynamics during pulsatile flow in a carotid artery bifurcation. *Computer Methods and Programs in Biomedicine*, *192*, p.105440.

[23] Lopes, D., Puga, H., Teixeira, J.C. and Teixeira, S.F., 2019. Influence of arterial mechanical properties on carotid blood flow: Comparison of CFD and FSI studies. *International Journal of Mechanical Sciences*, *160*, pp.209-218.

[24] Sia, S.F., Zhao, X., Yu, Y. and Zhang, Y., 2019. Multiphase particle-in-cell simulation in severe internal carotid artery stenosis. *Powder Technology*, *358*, pp.62-67.

[25] Lee, S.H., Han, K.S., Hur, N., Cho, Y.I. and Jeong, S.K., 2019. The effect of patient-specific non-Newtonian blood viscosity on arterial hemodynamics predictions. *Journal of Mechanics in Medicine and Biology*, *19*(08), p.1940054.

[26] Azar, D., Torres, W.M., Davis, L.A., Shaw, T., Eberth, J.F., Kolachalama, V.B., Lessner, S.M. and Shazly, T., 2019. Geometric determinants of local hemodynamics in severe carotid artery stenosis. *Computers in biology and medicine*, *114*, p.103436.

[27] Yao, X., Dai, Z., Zhang, X., Gao, J., Xu, G., Cai, Y. and Li, Z., 2019. Carotid Geometry as a Predictor of In-Stent Neointimal Hyperplasia—A Computational Fluid Dynamics Study—. *Circulation Journal*, *83*(7), pp.1472-1479.

[28] Kumar, N., Khader, A., Pai, R., Kyriacou, P., Khan, S. and Koteshwara, P., 2019. Computational fluid dynamic study on effect of Carreau-Yasuda and Newtonian blood viscosity models on hemodynamic parameters. *Journal of Computational Methods in Sciences and Engineering*, *19*(2), pp.465-477.

[29] Li, C.H., Gao, B.L., Wang, J.W., Liu, J.F., Li, H. and Yang, S.T., 2019. Hemodynamic factors affecting carotid sinus atherosclerotic stenosis. *World neurosurgery*, *121*, pp.e262-e276.

[30] Guerciotti, B. and Vergara, C., 2018. Computational comparison between Newtonian and non-Newtonian blood rheologies in stenotic vessels. *Biomedical Technology: Modeling, Experiments and Simulation*, pp.169-183.

[31] Domanin, M., Bissacco, D., Le Van, D. and Vergara, C., 2018. Computational fluid dynamic comparison between patch-based and primary closure techniques after carotid endarterectomy. *Journal of vascular surgery*, *67*(3), pp.887-897.

[32] Urevc, J., Žun, I., Brumen, M. and Štok, B., 2017. Modeling the effect of red blood cells deformability on blood flow conditions in human carotid artery bifurcation. *Journal of Biomechanical Engineering*, *139*(1), p.011011.

[33] Bit, A., Ghagare, D., Rizvanov, A.A. and Chattopadhyay, H., 2017. Assessment of influences of stenoses in right carotid artery on left carotid artery using wall stress marker. *BioMed research international*, *2017*(1), p.2935195.

[34] Conti, M., Long, C., Marconi, M., Berchiolli, R., Bazilevs, Y. and Reali, A., 2016. Carotid artery hemodynamics before and after stenting: A patient specific CFD study. *Computers & fluids*, *141*, pp.62-74.

[35] Gallo, D., Steinman, D.A. and Morbiducci, U., 2016. Insights into the co-localization of magnitude-based versus direction-based indicators of disturbed shear at the carotid bifurcation. *Journal of biomechanics*, *49*(12), pp.2413-2419.

[36] Sousa, L.C., Castro, C.F., António, C.C., Sousa, F., Santos, R., Castro, P. and Azevedo, E., 2016. Computational simulation of carotid stenosis and flow dynamics based on patient ultrasound data–A new tool for risk assessment and surgical planning. *Advances in Medical Sciences*, *61*(1), pp.32-39.

[37] Gharahi, H., Zambrano, B.A., Zhu, D.C., DeMarco, J.K. and Baek, S., 2016. Computational fluid dynamic simulation of human carotid artery bifurcation based on anatomy and volumetric blood flow rate measured with magnetic resonance imaging. *International Journal of Advances in Engineering Sciences and Applied Mathematics*, *8*, pp.46-60.

[38] Guerciotti, B., Vergara, C., Azzimonti, L., Forzenigo, L., Buora, A., Biondetti, P. and Domanin, M., 2016. Computational study of the fluid-dynamics in carotids before and after endarterectomy. *Journal of biomechanics*, *49*(1), pp.26-38.

[39] Siebert, M.W. and Fodor, P.S., 2009, October. Newtonian and non-newtonian blood flow over a backward-facing step–a case study. In *Proceedings of the COMSOL Conference, Boston* (Vol. 27).

[40] Molla, M.M. and Paul, M.C., 2012. LES of non-Newtonian physiological blood flow in a model of arterial stenosis. *Medical engineering & physics*, *34*(8), pp.1079-1087.

[41] Sinnott, M., Cleary, P.W. and Prakash, M., 2006, December. An investigation of pulsatile blood flow in a bifurcation artery using a grid-free method. In *Proc. Fifth International Conference on CFD in the Process Industries* (pp. 1-6).